

# Motion Planning for Small Formations of Autonomous Vehicles Navigating on Gradient Fields

Shahab Kalantar, Uwe Zimmer

Australian National University  
 Research School for Information Science and Engineering  
 and the Faculty for Engineering and Information Technology  
 Autonomous Underwater Robotics Research Group  
 Canberra, ACT 0200, Australia  
 shahab.kalantar@rsise.anu.edu.au | uwe.zimmer@ieee.org

**Abstract** – In this paper, we present a motion planning scheme for navigation of a contour-like formation of autonomous underwater vehicles on gradient fields and subsequent convergence to desired isoclines, inspired by evolution of closed planar curves. The basic evolution behaviour is modified to include moving boundary points and incorporate safety constraints on formation parameters. Also, the whole process is decomposed into a sequence of well-behaving states. As opposed to the basic model, the regularized solution is characterized by the maximum allowable curvature rather than balance of forces determined by fixed coefficients. Nevertheless, the proposed framework subsumes the original model. Blocking states and fairness are briefly discussed.

## I. INTRODUCTION

The need to deploy large numbers of autonomous vehicles to safely monitor underwater phenomena, which are usually of considerable spatial extent, is currently a driving impetus for many research efforts. These monitoring tasks include, among others, characterizing diffusion processes (e.g., temperature and salinity [2]) through the evolution of their *isoclines*, monitoring flows of one kind or another over *isobaths*, identification of *iso-tachs* of flow fields, and delineation of *boundaries* of plumes or biological concentrations. Due to inevitable uncertainties associated with measurements, any kind of imposed structure on the shape of vehicle formations can be of great help. Generally speaking, suitable formations will have to be *deformable* rather than rigid. They should have the capability to *lose* potential energy to get into the right *shape* and *gain* potential energy under the influence of ambient field gradients. Candidate formations are either dense networks (for area coverage [6],[7]) those resembling chains (for isocline tracking [5],[1],[8]) or both [3] (swarms with boundary). We will consider curved formations with open ends. The proposed strategy will ultimately be implemented on Serafina robots developed in our lab (figure 1). We will only consider the planar case where the robots are stabilized to navigate on an imaginary plane. In the following, we will precisely formulate the problem.

**Definition 1:** A field  $F$  is a continuously differentiable mapping  $F : D \otimes T \rightarrow \mathfrak{R}$ , where  $\mathfrak{R}$  denotes the real domain,  $D \subset \mathfrak{R}^2$  is the domain of definition of  $F$ , and  $T$  is some time domain. A **static field** is time-invariant in the period of time  $T$ , during which the field can be defined as  $F : \mathfrak{R}^2 \rightarrow \mathfrak{R}$  (we

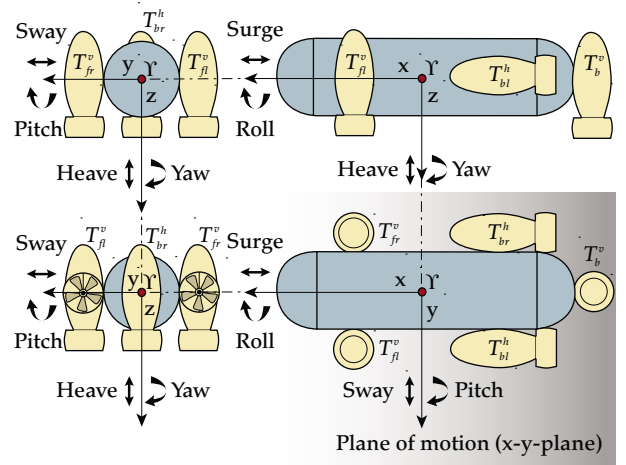


figure 1: Serafina, the plane of motion on which the robots behave like non-holonomic devices, as sway is not actuated. Refer to [12] for more information.

have extended  $D$  to the whole plane for simplicity). The **gradient** of  $F$  at  $q \in \mathfrak{R}^2$  is denoted by  $\nabla_q F(q)$  and defined as the vector  $[\partial/\partial x(F(q)), \partial/\partial y(F(q))]^T$ , expressed in some inertial coordinate frame  $\Upsilon = \{x, y\}$ .

**Definition 2:** For any fixed value  $F_d$ , such that  $\inf_{q \in \mathfrak{R}^2} F(q) \leq F_d \leq \sup_{q \in \mathfrak{R}^2} F(q)$ , a  **$F_d$ -level set (or isocline)** of  $F$  is defined by the equation  $F(q) = F_d$ . A level set is called a **level curve** if it is a single closed, simple and smooth ( $C^2$ ) curve  $\gamma_{F_d}^c : \varphi \rightarrow \mathfrak{R}^2$ . We simplify the notation to  $\gamma_{F_d} \cdot \gamma_{F_d}$  is parametrized by  $s \in \varphi$ , where  $\varphi \subset \mathfrak{R}$  is the parametrization domain (such as  $[0, 1]$ ).

For each such curve  $\gamma$ , at each point represented by  $s$ , a **Frenet-Serret frame**  $\Upsilon_\gamma(s) = \{\mathcal{N}_\gamma(s), \mathcal{T}_\gamma(s)\}$  can be defined, where  $\mathcal{T}_\gamma(s) = \dot{\gamma}(s)/\|\dot{\gamma}(s)\|$  is the unit *tangent vector* and  $\mathcal{N}_\gamma(s) = \mathcal{T}_\gamma(s)^\perp$  the unit *inward normal*. As the only information available to the robots is the value and local gradient of the field, the measure of *closeness* to an iso-cline is  $d_1(q, \gamma_{F_d}) = |F(q) - F_d|$  defined over  $Im(F) = F(D)$ , for  $q \in \mathfrak{R}^2$ , rather than Euclidian metric  $d_2(q, \gamma_{F_d}) = \|q - Q(q, \gamma_{F_d})\|$ ,  $Q(q, \gamma_{F_d})$  denoting the closest point on  $\gamma_{F_d}$  to  $q$ . The  $\varepsilon$ -neighborhood of a curve  $\gamma$  is denoted  $B_\varepsilon(\gamma)$  and is defined as  $B_\varepsilon(\gamma) = \{q \in \mathfrak{R}^2 \mid d_2(q, \gamma_{F_d}) \leq \varepsilon\}$

**Definition 3:** A **planar formation** is defined as a tuple  $R(t) = \{\{R_i\}, f(t), q^R(t)\}$ , where  $\{R_i\}$  denotes a collection of

$N$  robots (considered as point masses)  $R_i$ ,  $i = 0, \dots, N-1$ , with positions (states)  $q_i(t) \in \mathbb{R}^2$ , measured with respect to  $\Upsilon$ .  $q^R(t) = [q_0(t), \dots, q_{N-1}(t)]^T$  is the **collective state** of the formation.  $f(t) = [f_0(t), \dots, f_{N-1}(t)]^T$  is the **force** on the formation with the general form  $f_i(t) = f_i(\varphi_i(q^R(t)), \nabla_q F(q_i(t)))$ , where  $\varphi_i(t)$  is a projection operator. The equations of motion are  $\dot{q}_i(t) = f_i(t)$ , ignoring inertial effects.

**Problem 1:** Let  $R$  be a planar formation and  $\gamma_{F_d}$  the level curve corresponding to the level value  $F_d$  of a static field  $F$ . Let  $\Omega$  be an **admissible configuration space** and that  $\tilde{q}^R(t_0) \in \Omega$ . Find forces  $f_i$  such that for some finite time  $t_f$  and tolerance bound  $\varepsilon > 0$ , we have

1.  $\tilde{q}^R(t) \in \Omega$ ,  $\forall t \geq t_0$ , and
2.  $\forall t \geq t_f$ ,  $D(\tilde{q}^R(t), \tilde{B}_\varepsilon(\gamma_{F_d}))$  is as small as possible, where

$$\tilde{B}_\varepsilon(\gamma_{F_d}) \equiv \{\tilde{q} \in \Omega \mid \forall i, q_i \in B_\varepsilon(\gamma_{F_d})\} \quad (1)$$

and  $D(v, S)$  denotes the distance of  $v \in \Omega$  to the set  $S$ .

**Problem 2:** Let all the assumptions of problem 1 hold true. Assume that  $\tilde{q}^R(t_0) \in \tilde{B}_\varepsilon(\gamma_{F_d})$ . Find  $f_i$  such that

- $\forall t \geq t_0$ ,
1.  $\tilde{q}^R(t) \in \tilde{B}_\varepsilon(\gamma_{F_d})$ , and
2.  $\forall t_1 \geq t_0$ ,  $\exists t_2 > t_1$  such that for every  $i$ ,

$$\int_{t_1}^{t_2} \frac{\partial}{\partial t} \gamma^{-1}(Q(q_i(t), \gamma_{F_d})) \dot{Q}(q_i(t), \gamma_{F_d}) \dot{q}_i(t) > 0 \quad (2)$$

Assuming local *omni-directional* sensing, one straightforward way of approaching the first problem is to let every robot move towards the level set while exerting *repulsive* (and *attractive*) forces on each other for the purposes of *avoiding collisions* (maintaining *comfortable spacing*) and *maximal spreading* on the level curve, while maintaining *cohesion*. This approach can simply be implemented using the motion equations

$$\dot{q}_i(t) = -\beta_1(F(q_i(t)) - F_d) \nabla_q F(q_i(t)) - \sum_{j \in N_i(t)} \nabla_{q_i} U(q_i(t), q_j(t)) \quad (3)$$

where  $N_i(t)$  denotes a neighborhood around  $R_i$  and  $U(q_i, q_j)$  is a suitable repulsive-attractive potential. This is the gradient descent of the *cost function*

$$\sum_{i=0}^{N-1} \left[ d_1(q_i(t), \gamma_{F_d}) + \sum_{j \in N_i(t)} U(q_i, q_j) \right] \quad (4)$$

The equilibrium state is the result of local interactions and is a local minimum of

$$\frac{1}{2} \mathbf{Y}^T \mathbf{Y} + \sum_{i \neq j} U(q_i(t_f), q_j(t_f)) \quad (5)$$

where  $\mathbf{Y} = (F(q(t_f)) - F_d \mathbf{I}_N)$  and  $t_f$  is the time the equilibrium is attained, which *may not* be the desired final state. Obviously, we need more elaborate mechanisms, even with complete neighborhood sensing. In this paper, we start from a formation with a fixed topology, already shaped like an isocline, i.e., a *chain*, and use ideas from curve evolution. Such a formation is robust to large variations in gradient sensing and is suitable for more realistic directional sensors.

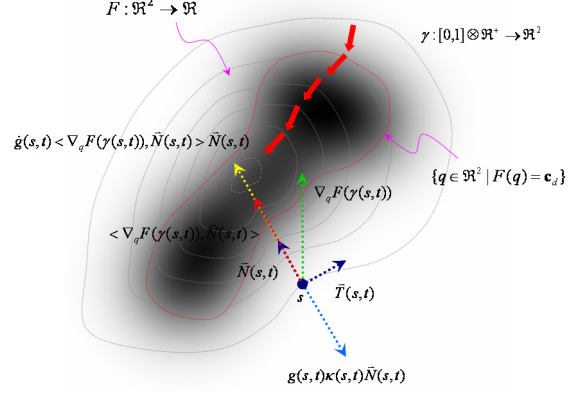


figure 2: Curve evolution

## II. CONTOUR FORMATIONS

**Definition 4:** A **virtual bi-directional communication channel** is a tuple  $C_{ij} = \langle R_i, R_j, \mu_i, \mu_j \rangle$ , where  $R_i, R_j \in \mathbb{R}$ ,  $\mu_i$  ( $\mu_j$ ) is a function computed by  $R_i$  ( $R_j$ ) and available to  $R_j$  ( $R_i$ ). Availability is realized by sending the value computed by  $\mu_i$  ( $\mu_j$ ) to  $R_j$  ( $R_i$ ) through some physical medium.

Note that this definition of a channel is an abstraction and can include active sensing, as well as ordinary communication.

**Definition 5:** A **contour formation** is a formation  $R$  together with virtual channels between each pair of neighboring robots  $C_{i-1,i} = \langle R_{i-1}, R_i, \mu_{i-1}, \mu_i \rangle$ ,  $i = 1, \dots, N-1$ , such that  $f_i(t) = f_i(q_i(t), \mu_{i-1}, \mu_{i+1}, \nabla_q F(q_i(t)))$ .

The robots  $R_{i-1}$  and  $R_{i+1}$  are called **left**, respectively **right neighbors** of  $R_i$ .  $R_0$  and  $R_{N-1}$  are called **end robots**. The pair  $l_i = \{q_{i-1}, q_i\}$  is called a **link**.

In a contour formation, robots are imagined as lying on an imaginary curve, forming a *polyline*. Each robot's position on the curve is determined by its index. According to the definition, a contour formation is *oriented* from left to right.

Let  $\gamma_R : [0, 1] \otimes T \rightarrow \mathbb{R}^2$  be a continuous curve residing in the plane, parametrized by  $s \in [0, 1]$ . Let  $\gamma_R(0, t) = \gamma_R(1, t)$  define the boundary condition if  $\gamma_R$  is closed and  $\dot{\gamma}_R(0, t) = \dot{\gamma}_R(1, t) = 0$  if it is open. At each point on the curve, fix the Ferrenet-Serret frame  $\Upsilon_s = \{\tilde{N}(s, t), \tilde{T}(s, t)\}$ , where  $\tilde{T}(s, t)$  is the unit tangent vector and  $\tilde{N}(s, t)$  the unit inward normal to the curve at that point. According to curve evolution theory, the partial differential equation

$$\dot{\gamma}_R(s, t) = g(s, t) \kappa(s, t) \tilde{N}(s, t) - \langle \nabla_{\Upsilon} g(F(\gamma_R(s, t))), \tilde{N}(s, t) \rangle \tilde{N}(s, t) \quad (6)$$

gives the steepest descent for the energy functional

$$\int_0^1 g(\gamma(s, t)) ds \quad (7)$$

where  $g : \mathbb{R} \rightarrow [0, 1]$ ,  $F \rightarrow g(F)$ , is a monotonically increasing function of  $F(\gamma_R(s, t)) - F_d$ , i.e.,  $g(F(\gamma_R(s, t))) \rightarrow 0$  as  $F(\gamma_R(s, t)) \rightarrow F_d$  and  $g(F(\gamma_R(s, t))) \rightarrow 1$  as  $|F(\gamma_R(s, t)) - F_d| \rightarrow \infty$ . Also,  $\kappa(s, t)$  is the curvature at  $s$  (see figure 2). Refer to [4] for details of general curve evolution theory.

Straightforward translation of the above motion equation to the case of contour formations would result in the following form for the forces acting on each robot in the formation:

$$f_i(t) = \beta_1 \kappa_i(t) g(F(q_i(t))) \tilde{N}_i(t) - \beta_2 \dot{g}(F(q_i(t))) \langle \nabla_q F(q_i(t)), \tilde{N}_i(t) \rangle \tilde{N}_i(t) \quad (8)$$

Here,  $\kappa_i(t)$  denotes a discrete approximation of the curvature of the polyline defining the formation and is given by

$$\kappa_i(t) = \text{acos} \left( \frac{\langle q_{i+1} - q_i, q_i - q_{i-1} \rangle}{\|q_{i+1} - q_i\| \|q_i - q_{i-1}\|} \right) \frac{\tilde{\kappa}_i(t)}{\|q_{i+1} - q_{i-1}\|} \quad (9)$$

where  $\tilde{\kappa}_i(t) = \text{sign}(\langle q_{i+1} - q_i, q_i - q_{i-1} \rangle)$ . Note that there are other ways of defining the curvature. The inward normal vector is defined as  $\tilde{N}_i(t) = \tilde{T}_i(t)^\perp$  where

$$\tilde{T}_i(t) = \frac{q_{i+1} - q_{i-1}}{\|q_{i+1} - q_{i-1}\|} \quad (10)$$

is the tangent vector at  $q_i(t)$  (see figure 3). Also define

$$g(F) = 1 - \frac{1}{1 + \sigma(F - F_d)^2} \quad (11)$$

For the end robots, we define

$$T_0(t) = \frac{q_1(t) - q_0(t)}{\|q_1(t) - q_0(t)\|} \quad (12)$$

$$T_{N-1}(t) = \frac{q_{N-1}(t) - q_{N-2}(t)}{\|q_{N-1}(t) - q_{N-2}(t)\|} \quad (13)$$

such that  $\tilde{N}_0(t) = T_0(t)^\perp$  and  $\tilde{N}_{N-1}(t) = T_{N-1}(t)^\perp$ . Moreover,  $\kappa_0(t) = -\kappa_1(t)$  and  $\kappa_{N-1}(t) = -\kappa_{N-2}(t)$ . Refer to [8] for justification of these definitions. Note that this *Lagrangian* scheme (in the case of closed curves) would solve the *rendezvous* problem, i.e., the robots will eventually converge to a single point. To distribute the robots along the imaginary curve representing the formation, we need a non-zero tangential force as well. Accordingly, we propose the general form

$$f_i(t) = b(f_{N_i}(t)) \tilde{N}_i(t) + b(f_{T_i}(t)) \tilde{T}_i(t) \quad (14)$$

where  $b: \mathcal{R} \rightarrow I$  is some suitable bounding function. Now, problem 1 reduces to the design of  $f_N(t)$  and  $f_T(t)$ . To ad-

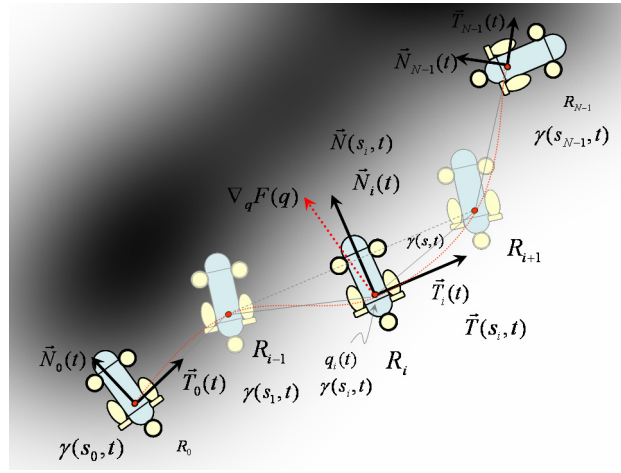


figure 3: Contour formation

dress problems 1 and 2, we propose the following general forms

$$f_{N_i}(t) = f_{F_i}(t) + f_{\kappa_i}(t) \quad (15)$$

$$f_{T_i}(t) = f_{V_i}(t) + f_{C_i}(t) \quad (16)$$

$f_{F_i}(t)$  is the *external* force due to the local gradient, pulling the formation towards the boundary.  $f_{\kappa_i}(t)$  is the *internal* compensating force which tries to *smooth* the formation.  $f_{V_i}(t)$  is the *distributing* force making sure that the robots are evenly distributed along the imaginary curve, subject to some constraint on the total length. Finally,  $f_{C_i}(t)$  is a force which makes the formation slide on the boundary. We propose to decompose these forces into different multiplicative factors, each defining a particular function. The general form is  $f_r(t) = \beta_r \alpha_r(t) \xi_r(t) \eta_r(t)$  where  $r \in \{F_i, \kappa_i, V_i, C_i\}$ .  $\eta_r(t)$  denotes a *basic behaviour* which in our case will be as simple as a direction of motion.  $\beta_r$  is a fixed *proportionality factor* which is a-priori defined by the designer.  $\xi_r(t)$  denotes the *magnitude* of the corresponding basic behaviour which reflects the quality of motion.  $\zeta_r(t) = \beta_r \xi_r(t) \eta_r(t)$  designates the *target dynamics*. Finally,  $\alpha_r: \mathcal{R} \times T \rightarrow [0, 1]$ ,  $\zeta_r(t) \rightarrow \alpha_r(t)$ , represents the solution to the *activation dynamics*, which together with target dynamics, constitute the *dual dynamics* approach [10].

**Definition 6:** A formation  $R$  is called **free** if  $\nabla_q F(q) \equiv 0$  for every  $q \in \mathcal{R}^2$ . Alternatively, we may put  $\xi_{F_i}(t) = 0$ . Otherwise,  $R$  is called **forced**.  $R$  is called **un-constrained** if  $\alpha_r(t) = 1$  at all times. Otherwise, it is called **constrained**.

We define

$$\eta_{F_i}(t) = -\text{sign}(F(q_i(t)) - F_d) \quad (17)$$

$$\xi_{F_i}(t) = \frac{2\sigma|F(q_i(t)) - F_d|}{(1 + \sigma(F - F_d)^2)^2} \langle \nabla_q F(q_i(t)), \tilde{N}_i(t) \rangle \xi_{B_i}(t) \quad (18)$$

For the internal force, define

$$\eta_{\kappa_i}(t) = \tilde{\kappa}_i(t) \quad (19)$$

$$\xi_{\kappa_i}(t) = (\tau_f g(F(q_i(t))) + (1 - \tau_f)) |\kappa_i(t)| \xi_{B_i}(t) \quad (20)$$

where  $\tau_f$  is 1 if the formation is forced and 0 otherwise.  $\xi_{B_i}(t)$  is a *balancing* factor which gives priority to tangential motion over normal motion. Regarding the redistribution force, we proposed the following:

$$\eta_{V_i}(t) = \text{sign}(e_{i,i+1} - e_{i,i-1}) \quad (21)$$

$$\xi_{V_i}(t) = |e_{i,i+1} - e_{i,i-1}| \left( 1 - e^{-\|e\|^2 / \sigma^2} \right) \quad (22)$$

where

$$e_i = E_{i,i+1}(t) - E_{i,i-1}(t) \quad (23)$$

$$E_{i,i\omega 1}(t) = \frac{1}{2} e_{i,i\omega 1}^2 \quad (24)$$

and  $e_{i,i\omega 1} = \|q_{i\omega 1} - q_i\| - d$ ,  $\omega \in \{-, +\}$ . Here,  $d$  is a desired pre-defined inter-robot distance.  $\xi_{B_i}(t)$  can now be defined as a monotonically decreasing function of  $|e_{i,i+1} - e_{i,i-1}|$ . For the end robots, define

$$e_0 = E_{0,1}(t), e_{N-1}(t) = -E_{N-1,N-2}(t) \quad (25)$$

$$e_{N-1,N} = e_{-1,0} = 0 \quad (26)$$

Note that for interior robots,

$$e_{i,i+1} - e_{i,i-1} = \|q_{i+1} - q_i\| - \|q_i - q_{i-1}\| \quad (27)$$

which means that these robots can only maintain equal distances with their neighbours (even distribution). The actual length constraint has to be enforced via the motions of the end robots.

As will be seen in the simulation section, the un-constrained model does not respect some required safety (collision) issues which may jeopardize the mission. Activation dynamics is treated in next section.

### III. CONSTRAINTS

Let's first define some relevant configuration spaces defining a contour formation.

**Definition 7:** A contour formation is called **simple** if it has no self-intersections. In other words, for every two distinct segments  $l_i = \{q_i, q_{i+1}\}$  and  $l_j = \{q_j, q_{j+1}\}$  such that  $j+1 \neq i$  and  $i+1 \neq j$ , the expressions  $(q_{i+1} - q_i) \cdot (q_{j+1} - q_j)^\perp$ ,  $(q_{j+1} - q_j) \cdot (q_i - q_{i-1})^\perp$  and  $(q_{i+1} - q_i) \cdot (q_i - q_{i-1})^\perp$  are not zero at the same time, and either

1.  $(q_{i+1} - q_i) \cdot (q_{j+1} - q_j)^\perp = 0$ , or
  2.  $(q_{j+1} - q_j) \cdot (q_i - q_{i-1})^\perp \notin [0, 1]$
- and  $(q_{i+1} - q_i) \cdot (q_i - q_{i-1})^\perp \notin [0, 1]$ .

We denote the space of all simple formations by  $\Omega_S$ .

**Definition 8:** Formation  $R$  is called **proper** if for

every  $i = 1, \dots, N-2$ ,  $\hat{x}_{i-1} \leq \hat{x}_i \leq \hat{x}_{i+1}$  where  $\hat{x}_i$  denotes the  $x$ -component of  $R_z^T(\theta_j)q_j$  where  $R_z^T(\theta_j)$  is the inverse rotation around  $z$  axis by

$$\theta_j = \text{atan}\left(\frac{y_{j+1} - y_{j-1}}{x_{j+1} - x_{j-1}}\right) \quad (28)$$

The space of all proper formations is denoted  $\Omega_P$ .

**Definition 9:** The formation  $R$  is called  $[d_1, d_2]$ -**distance bounded** if for every pair  $R_i$  and  $R_{i+1}$ , we have  $d_1 \leq \|q_i - q_{i+1}\| \leq d_2$ .  $\Omega_{[d_1, d_2]}$  denotes the space of all such formations.

**Definition 10:** The formation  $R$  is called  $\kappa_M$ -**curvature bounded** if for every  $R_i$ , we have  $|\kappa_i| \leq \kappa_M$ .  $\Omega_{\kappa_M}$  denotes the space of all such formations.

**Definition 11:** A formation  $R$  is called  $\{[d_1, d_2], \kappa_M\}$ -**valid** at time  $t$  if  $q^R(t) \in \Omega_V$ , where  $\Omega_V = \Omega_S \cap \Omega_P \cap \Omega_{\kappa_M} \cap \Omega_{[d_1, d_2]}$ .  $R$  is called **perturbed** otherwise.

In this paper, for the sake of simplicity, we assume that the formation will always stay in  $\Omega_S \cap \Omega_P$ .

**Definition 12:** A perturbed formation  $R$  is called  $\{\varepsilon_\kappa, \varepsilon_d\}$ -**bounded** if  $q^R(t) \in \Omega_S \cap \Omega_P$  and for every  $i$ ,

$$|\kappa_i(t)| \leq (\kappa_M + \varepsilon_\kappa) \quad (29)$$

$$(d_1 - \varepsilon_d) \leq \|q_i - q_{i+1}\| \leq (d_2 + \varepsilon_d) \quad (30)$$

$\Omega$  in Problem 1 can now be replaced with  $\Omega_V$  for some given  $[d_1, d_2]$  and  $\kappa_M$ .

Regarding self-intersections, let  $\gamma$  be a given open curve on the plane with fixed length  $l(\gamma)$ . Imagine  $\gamma$  forming a circle such that the end points are touching. Such a circle is actually the *osculating circle* of the curve with *radius of curvature* equal to  $r = l(\gamma)/2\pi$ . The curvature is given by

$$|\kappa_\gamma(s)| = \left| -\frac{1}{r} \cos\left(\frac{s}{r}\right) \hat{i} - \frac{1}{r} \sin\left(\frac{s}{r}\right) \hat{j} \right| = \frac{1}{r} = \frac{2\pi}{l(\gamma)} \quad (31)$$

We denote this curvature by  $\kappa_M^*$ . It is obvious that, while in this configuration, any curvature greater than this will cause the curve to self-intersect itself. In other words, a *necessary* condition for intersection is that  $|\kappa_\gamma(s)| > \kappa_M^*$ , for some  $s \in [0, 1]$ . For a formation, we can set  $l(R) = (N-1)d_2$ . This is, of course, not a *sufficient* criterion. In principle, to avoid anomalous situations, a formation should start with lower values for  $\kappa_M$  and relax to higher allowable values when *sufficiently close* to the boundary.

**Definition 13:** Let  $h: \Omega \rightarrow \mathfrak{R}$  be a continuous mapping. A **constraint**  $\tilde{g}$  is defined by the inequality  $g(h(q)) \leq 0$  for every  $q \in \Omega$ , where  $g: \mathfrak{R} \rightarrow \mathfrak{R}$ . Let  $\varepsilon > 0$  be given.  $\tilde{g}$  is called  $\varepsilon$ -**safe** if  $g(h(q)) \leq -\varepsilon$ .  $\tilde{g}$  is called  $\varepsilon$ -**unsafe** if  $g(h(q)) > \varepsilon$ . It is called  $\varepsilon$ -**critical** if  $-\varepsilon < g(h(q)) < \varepsilon$ . Finally,  $\tilde{g}$  is called  $\varepsilon$ -**enabled** if  $-\varepsilon < g(h(q))$ .

See [11] for similar definitions. Here, we deal with simple constraints of the form  $g(t) = h(q) - c$  (**type I**) and  $g(t) = c - h(q)$  (**type II**). For every  $i = 0, \dots, N-1$ , three constraints are defined:

1.  $\tilde{g}_{d_{1,i}}$  with  $g_{d_{1,i}}(t) = d_1 - \|h_{d_i}(q)\|$ , where  $h_{d_i}(q) = q_i(t) - q_{i-1}(t)$ .
2.  $\tilde{g}_{d_{2,i}}$  with  $g_{d_{2,i}}(t) = \|h_{d_i}(q)\| - d_2$  and  $h_{d_i}(q)$  as above.
3.  $\tilde{g}_{\kappa_i}$  with  $g_{\kappa_i}(t) = |h_{\kappa_i}(q)| - \kappa_M$ , where  $h_{\kappa_i}(q) = \kappa_i(q_{i-1}, q_i, q_{i+1})$ .

Note that the general form of a constraint is  $t_{\tilde{g}}(h(q) - c)$ , where  $t_{\tilde{g}}$  is 1 for **type I** constraints and is  $-1$  for **type II** constraints. If  $v_i(t)$  denotes the velocity vector of  $R_i$ , then it should be in the direction of satisfaction of the above constraints. If a condition  $g$  is satisfied by  $v_i(t)$  at time  $t$ , we denote it by  $v_i(t) \perp \tilde{g}$ . Otherwise, we will use the notation  $v_i(t) \parallel \tilde{g}$ .

Define the Lyapunov function

$$V_h(t) = \frac{1}{2}(h(t))^2 \quad (32)$$

such that

$$\frac{\partial}{\partial q_i} V_h(t) = h(q) \frac{\partial}{\partial q_i} h(q) \quad (33)$$

which always in the direction of violation of the constraint. For  $v_i(t) \perp \tilde{g}$ , we should either have  $g(h(q)) \leq 0$  or

$$v_i(t) \frac{\partial}{\partial q_i} V_h(t) \leq 0 \quad (34)$$

If we define

$$z_{\tilde{g},i}(t) = t_{\tilde{g}} u(g(f(q))) \frac{\partial}{\partial q_i} V_f(t) \quad (35)$$

then we should have  $z_{\tilde{g},i}(t)^T v_i(t) \leq 0$ .

Every force  $f_p(t)$ ,  $\rho \in \{F_i, \kappa_i, V_i\}$  is involved in seven constraints  $\tilde{g}_{d_{1,i}}$ ,  $\tilde{g}_{d_{1,i+1}}$ ,  $\tilde{g}_{d_{2,i}}$ ,  $\tilde{g}_{d_{2,i+1}}$ ,  $\tilde{g}_{\kappa_i}$ ,  $\tilde{g}_{\kappa_{i-1}}$  and  $\tilde{g}_{\kappa_{i+1}}$ .

The terms  $\alpha_p(t)$ , should deactivate  $\zeta_p(t)$  when the corresponding constraint is enabled, in a continuous way. We take  $\alpha_p(t)$  to be a combination

$$\begin{aligned} \alpha_r(t) &= \widehat{\alpha}_{\rho, \tilde{g}_{d_{1,i}}}(t) \oplus \widehat{\alpha}_{\rho, \tilde{g}_{d_{2,i}}}(t) \oplus \widehat{\alpha}_{\rho, \tilde{g}_{\kappa_i}}(t) \\ &\oplus \widehat{\alpha}_{\rho, \tilde{g}_{d_{1,i+1}}}(t) \oplus \widehat{\alpha}_{\rho, \tilde{g}_{d_{2,i+1}}}(t) \\ &\oplus \widehat{\alpha}_{\rho, \tilde{g}_{\kappa_{i-1}}}(t) \oplus \widehat{\alpha}_{\rho, \tilde{g}_{\kappa_{i+1}}}(t) \end{aligned} \quad (36)$$

where  $\widehat{\alpha}_{\rho, \tilde{g}}(t)$  is responsible for constraint  $\tilde{g}$  and the operator  $\oplus$  is simple multiplication or minimum-taking.  $\widehat{\alpha}_{\rho, \tilde{g}}(t)$  is defined as

$$\widehat{\alpha}_{\rho, \tilde{g}}(t) = 1 - \alpha_{\rho, \tilde{g}}(t) \quad (37)$$

where  $\alpha_{\rho, \tilde{g}}(t) = v_\alpha \tanh(\beta_\alpha \alpha_{\rho, \tilde{g}}^\omega(t))$

$\alpha_{\rho, \tilde{g}}^\omega(t)$  being the solution of a differential equation

$$\dot{\alpha}_{\rho, \tilde{g}}^\omega(t) = \mathfrak{S}\left(\alpha_{\rho, \tilde{g}}(t), \frac{\partial}{\partial q_i} V_f(t), g(f(q))\right) \quad (38)$$

We propose the following form for

$\mathfrak{S}$ :

$$\begin{aligned} \dot{\alpha}_{\rho, \tilde{g}}^\omega(t) &= \chi_{\rho, \tilde{g}}^\omega(t) \chi_{\rho, \tilde{g}}^\delta(t) \\ &- \beta(1 - \chi_{\rho, \tilde{g}}^\delta(t)) \alpha_{\rho, \tilde{g}}(t) - \beta(1 - \chi_{\rho, \tilde{g}}^\omega(t)) \alpha_{\rho, \tilde{g}}(t) \end{aligned} \quad (39)$$

$\chi_{\rho, \tilde{g}}^\delta(t)$  activates inhibition when the constraint is enabled and is given by

$$\chi_{\rho, \tilde{g}}^\delta(t) = \sigma_{-\varepsilon, \beta}(g(f(q))) \quad (40)$$

where the function  $\sigma_{-\varepsilon, \beta, \varepsilon}(x)$  (figure 4) is defined by  $\sigma_{-\varepsilon, \beta, \varepsilon}(x) = \sigma_{-\varepsilon, \beta}(x)$  when

$\varepsilon < \sigma_{-\varepsilon, \beta}(x) < 1 - \varepsilon$ , is zero when  $\sigma_{-\varepsilon, \beta}(x) \leq \varepsilon$ , and 1 when  $\sigma_{-\varepsilon, \beta}(x) \geq 1 - \varepsilon$ . Here,  $\sigma_{p, q}(x) = (1 + e^{-4q(x-p)})^{-1}$ .  $\chi_{\rho, \tilde{g}}^\omega(t)$  activates inhibition only when the direction of motion is towards the violation of the constraint and the angle between the velocity and the direction of decrease is less than some threshold and is given by

$$\chi_{\rho, \tilde{g}}^\omega(t) = \sigma_{\varepsilon_\phi, \beta} \left( t_{\tilde{g}} \frac{\frac{\partial}{\partial q_i} V_f(t)^T}{\left\| \frac{\partial}{\partial q_i} V_f(t) \right\|} \frac{\zeta_p(t)}{\|\zeta_p(t)\|} \right) \quad (41)$$

#### IV. SUPERVISORY CONTROL

Figure 5(a) shows the block diagram of the control system for a single robot. locks  $B_\alpha$  calculate the basic behaviour (as described in section 2), while blocks  $D_\alpha$  produce constrained behaviour. The general structure of  $D_\alpha$  blocks is shown in figure 5(b). A *higher-level supervisor* (e.g., humans) provides the desired values for  $\kappa_M$ ,  $d_1$ ,  $d_2$  and  $F_d$ . The role of blocks  $\Theta_{\{\kappa_M\}}$ ,  $\Theta_{\{B_\kappa\}}$  and  $\Theta_{\{B_F\}}$  will be explained later on. Note that the flow of data is modified at some points depending on the current state  $s(t)$  of a *supervisory controller*  $s$ , modelled as a *hybrid* state transition diagram

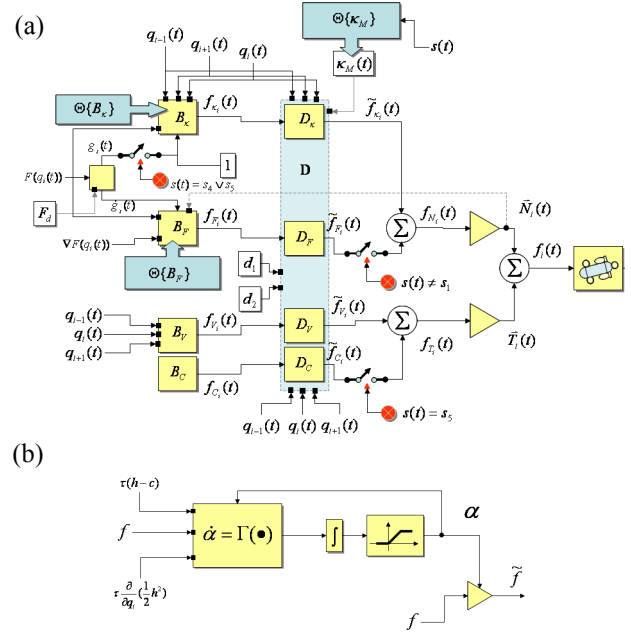


figure 5: (a) Controller block diagram, (b) activation strength

and depicted in figure 6(a). This controller is the core of our proposed motion planning scheme. Every robot maintains a copy of this controller. As will be explained in a moment, it requires some global knowledge about the state of the whole formation which can be gained through some form of *consensus*. We will not discuss this *synchronization* mechanism in this paper; refer to [9] for possible approaches. It is also operated by commands from the higher-level supervisor. For the sake of clarity, it is assumed that all the robots receive these commands instantaneously. All of the robots are initially in state  $s_1$  (*smoothing*). The command *cmd\_START* initiates formation evolution. In the initial state, the curvature-based and the tangential distribution forces are the only active ones and serve to *usher* the formation into the safe region (described below) without the influence of the disruptive gradient field. Now, denote by  $j^*$  the index of the robot with the largest absolute curvature. When  $\kappa_{j^*}(t)$  falls below some *smoothness* limit  $\kappa_M^s - \varepsilon_s$ , the controller transitions to state  $s_2$  (*marching*) which switches the field force on. After a finite amount of time, the potential energy  $P$  of the formation

$$P = \sum_{i=0}^{N-1} |\zeta_{F_i}(t) - \zeta_{\kappa_i}(t)| \quad (42)$$

will converge to a very small value  $\delta_s$  at which point the field and curvature forces have balanced each other and the formation is sufficiently close to the iso-cline. The curvature limit is now, after entering  $s_3$  (*adaptation*), set to  $\kappa_M^d$ . After stabilization, it would now be safe to switch to state  $s_4$  (*attachment*) and weight the curvature force by  $g(t)$  which will effectively drag the formation to the iso-cline. This may place the formation at the boundary of the safe region. The command *cmd\_DETACH* can be used to *disentangle* the formation from the iso-cline. Finally, when *cmd\_SLIDE* is

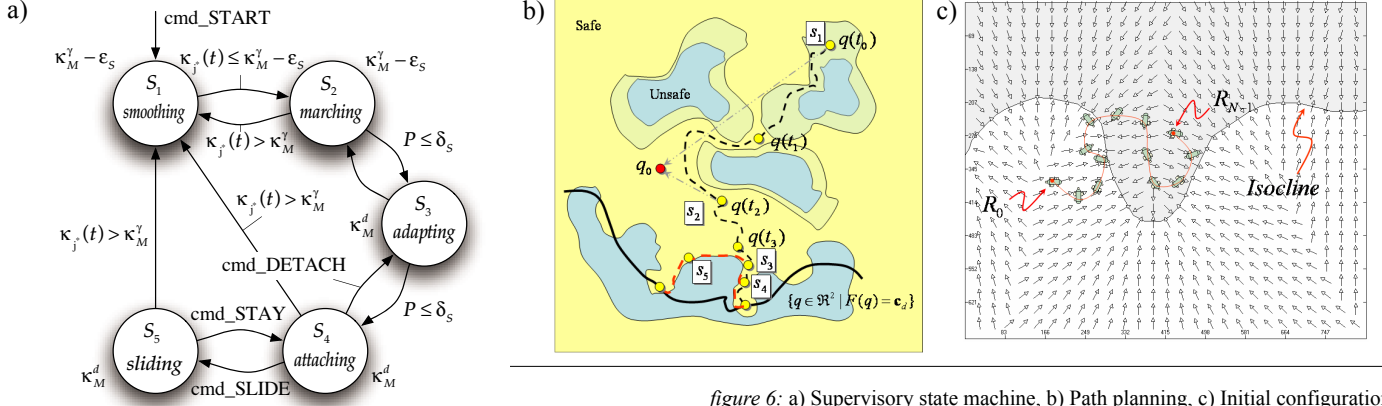


figure 6: a) Supervisory state machine, b) Path planning, c) Initial configuration

along the iso-cline. Figure 6(b) shows graphically the process outlined above.

Block  $D$  ensures *safety* but contour formations are an example of constrained mechanical multi-body systems and as such can get stuck in *blocking states*, depending on the value of  $\kappa_M$ . Mechanisms for escaping these states will make the system a *fair* one. We will examine each of the cases. In state  $S_1$ , the formation may initially be so far from the safe region that it may not even move. One solution to this problem is to relax the constraint on curvature enough to increase the mobility. This is exactly what  $\Theta\{\kappa_M\}$  does and will be discussed in more detail shortly. Another complementary solution can be arrived at by considering the fact that the robots at and near the ends are only aware of the local curvature. If their curvature is artificially defined to encompass a larger neighborhood, then their motion will help increase the mobility of inner robots with higher curvatures. Such a scheme should be effected by block  $\Theta\{B_\kappa\}$  but, due to space limitations, will not be pursued in detail. The particular scheme we use in the simulations is that  $\Theta\{B_\kappa\}$  adds to the curvature of every robot (with  $\kappa_i(t) \leq \kappa_\delta$ ) an additional value  $\tilde{\kappa}_i(t)$  which is equal to the next  $\kappa_{i+n}(t) > \kappa_\delta$  if for every  $j < i$ ,  $\kappa_j(t) \leq \kappa_\delta$ , and similarly for the other direction.

In state  $S_2$ , if  $\kappa_M^y - \epsilon_s$  is too low, the field force may be hindered altogether. Thus, it should be selected high enough or  $\Theta\{\kappa_M\}$  be used to relax it (not exceeding  $\kappa_M^y$ ) if needed. Likewise, in state  $S_5$ , a very low  $\kappa_M^d$  may hinder  $f_c(t)$  and can be treated as above.

Another blocking situation while in state  $S_2$  is being stuck in an undesired local minimum. For good adaptation, it is necessary that the formation be *oriented* towards the iso-cline. This means that for all the robots,  $\nabla F(q_i)$  should be almost aligned with  $N_i$ .  $\Theta\{B_\kappa\}$  is responsible for producing a modified artificial field force to make sure this happens before entering  $S_3$ . We will not discuss it here.

While in  $S_1$ ,  $\Theta\{\kappa_M\}$  gradually adjusts  $\kappa_M$  such that  $\alpha_{\kappa_j}$  is greater than a given mobility level  $M_l$  using

$$\frac{d}{dt}\kappa_M(t) = -\Delta(\alpha_{\kappa_j}(t) - M_l) \quad (43)$$

This will give the formation just enough mobility to proceed, while bounding the maximum curvature.  $\kappa_M$  is further constrained to the range  $[\kappa_M^{\min}, \kappa_M^{\max}]$ .

## V. SIMULATION RESULTS

In this section, we present some simulation runs which delineate the similarities and differences of the original and the constrained model. In all the simulations, the robots move in an artificially produced force field. At each location, the force (represented by an arrow) simulates a gradient and is computed as the output of a Gaussian function of the distance to the closest point to the iso-cline (represented as a line cutting the plane into two distinct areas). In all the simulations, we have set  $d_2 = 80$ ,  $d_1 = 50$ . The upper and lower limits for  $\kappa_M$  are, respectively,  $\kappa_M^d = 0.03$  and  $0.001$ . Also,  $\beta_F = 10^8$ ,  $\beta_\kappa = 10^5$ ,  $\beta_V = 10^5$ . Figure 6(c) shows the initial configuration used for all the runs. Note that  $\kappa_M^y = 0.00654$ . Figure 7(a) shows the adaptation of the formation to the iso-cline according to the original model. Figure 7(b) and 7(c) show the evolution of the curvatures and the distances. Note the high curvatures and proximities. Figure 8(a) shows the trace of the *un-forced* formation moving according to the original model, while in figure 8(b) and 8(c) are shown the evolution of the curvature and distance for each robot. While an improvement in itself, figure 9 shows the performance of the un-forced constrained formation with relaxation, where  $\Delta = 0.001$  and  $M_l = 0.3$ . Note that the maximum curvature attained is much lower and distance bounds are well respected. Here, we have chosen  $\kappa_M^{\min} = 0.001$  and  $\kappa_M^{\max} = 0.03$ . In this run,  $\kappa_M$  is saturated at  $0.03$  most of the time. Figure 10(a) and 10(b) show, respectively, the adaptation after switching the field force on and the evolution of curvature of the constrained model after attachment. Figure 11 shows the performance when  $\Theta\{B_\kappa\}$  is also active. Note the maximum curvature and, particularly, the increased speed of convergence. Finally, figure 12 shows the evolution of curvature and  $\kappa_M$  when  $\Theta\{\kappa_M\}$  and  $\Theta\{B_\kappa\}$  are both active and  $M_l = 0.3$  and  $\Delta = 0.001$ . Note that due to a tight bound on  $\kappa_M$ , parts (actually, the ends) of the formation have to go through a long manoeuvre but the curvatures are kept within strict bounds. Without relaxation, the curvatures would be non-increasing, convergence only relying on the motion of end robots.

## VI. CONCLUSIONS AND FUTURE RESEARCH

In this paper, we proposed a framework for planning the motion of a group of planar autonomous agents in a chain formation for the purposes of adaptation to level curves of environmental fields using local measurements and communication. The framework is composed of a hybrid supervisory automaton, a block generating the basic behaviour according to a discrete implementation of the original curve evolution scheme, a governor block constraining the basic behaviour to admissible regions (ensuring formation safety within some user-determined bounds) and three blocks modifying the basic behaviour (to ensure fairness of the system). The overall strategy is to make the formation smooth enough before exposing it to external forces and then decrease the internal force when safely close to the iso-cline. Of the three fairness blocks, the one which acts by relaxing the curvature constraint was discussed in detail. The other two will be explored in future papers to make the framework complete. Among the topics to be addressed in subsequent research are distributed gradient estimation, effects of sensor noise, directional sensing, effective consensus protocols, considering the non-holonomicity of the vehicles, characterization of the underlying diffusion process, and more detailed study of mobility of formation in each state.

## REFERENCES

- [1] Kalantar, S., Zimmer, U., *Contour Shaped Robotic Formations for Isocline Adaptation*, Proc. of the intl. conf TAROS '05, London, U.K., 2005.
- [2] Okubo, A., *Diffusion and Ecological Problems: Mathematical Models*, Vol. 10 in Biomathematics Series, Springer-Verlag, 1980.
- [3] Kalantar, S., Zimmer, U., *Distributed Shape Control of Homogeneous Swarms of Autonomous Underwater Vehicles*, To appear in *Autonomous Robots*, 2006.
- [4] Caselles, V., Kimmel, R., Sapiro, G., *Geodesic Active Contours*, Intl. Journal of Computer Vision, Vol. 22, No. 1, 1997.
- [5] Marthaller, D., Bertozzi, A.L., *Tracking environmental level sets with autonomous vehicles*, Proc. of the Conf. on Cooperative Control and Optimization, Gainesville, Florida, Dec. 2002.
- [6] Cortes, J., Martinez, S., Karatas, T., Bullo, F., *Coverage Control for Mobile Sensing Networks*, in Proc. of IEEE Int. Conf. on Robotics and Automation, 2002.
- [7] Shucker, B., Bennett, J.K., *Scalable Control of Distributed Robotic Macrosensors*, 7th Int. Symp. on Dist. Autonomous Robotic Systems, June 2004.
- [8] Kalantar, S., Zimmer, U., *Control of Open Contour Formations of Autonomous Underwater Vehicles*, International Journal of Advanced Robotic Systems, Vol.2, No. 4, Dec. 2005.
- [9] Ren, W., Beard, R.W., Atkins, E.M., *A Survey of Consensus Problems in Multi-Agent Coordination*, American Control Conference, Portland, USA, 2005.
- [10] Jaeger, H., Christaller, T., *Dual Dynamics: Designing Behaviour Systems for Autonomous Robots*, Artificial Life and Robotics, Vol. 2, 1998.
- [11] Pereira, G.A.S., Das, A.K., Kumar, V., Campos, M.F.M., *Formation Control with Configuration Space Constraints*, Proc. of IEEE/RJS Intl. Conf. on Intelligent Robots and Systems, Las Vegas, USA, 2003.
- [12] <http://serafina.anu.edu.au/>

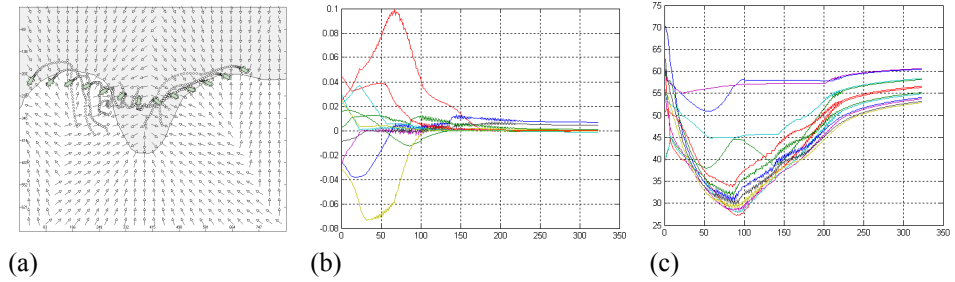


figure 7: Original model. (a) Trace, (b) Curvature evolution, (b) Distance evolution

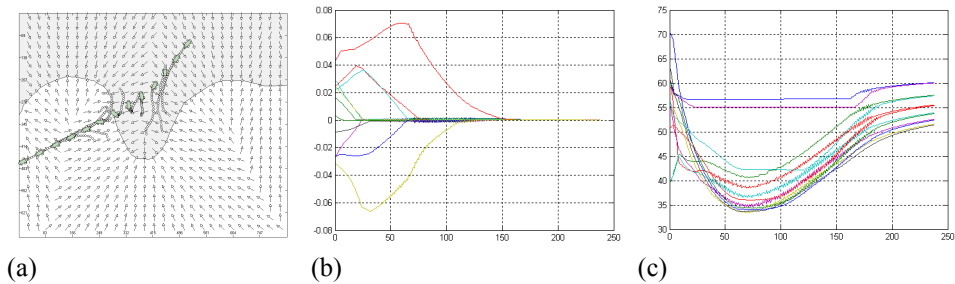


figure 8: (a) Final configuration, (b) Curvature evolution, (c) Distance evolution

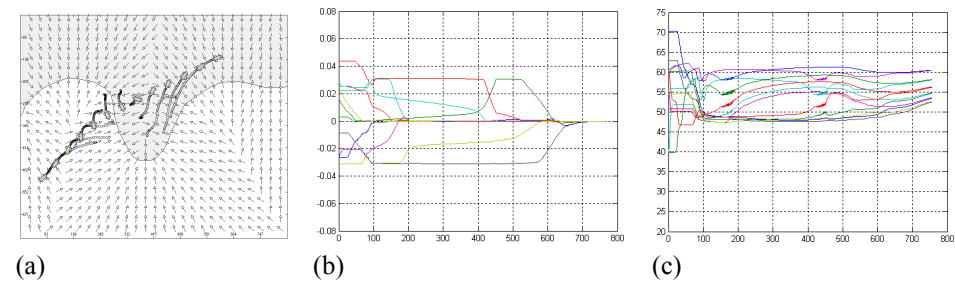


figure 9: (a) trace, (b) Curvature evolution, (c) Distance evolution.

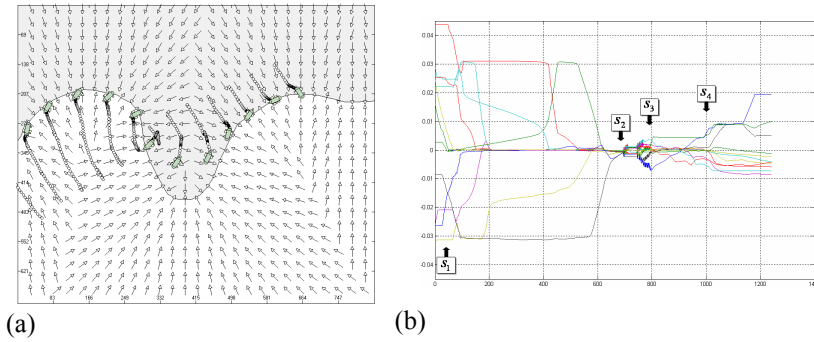


figure 10: (a) Force balance after adaptation, (b) The whole cycle

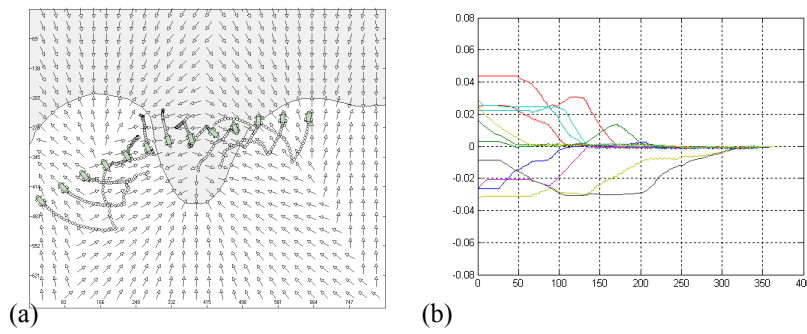


figure 11: Relaxation plus improved curvature definition

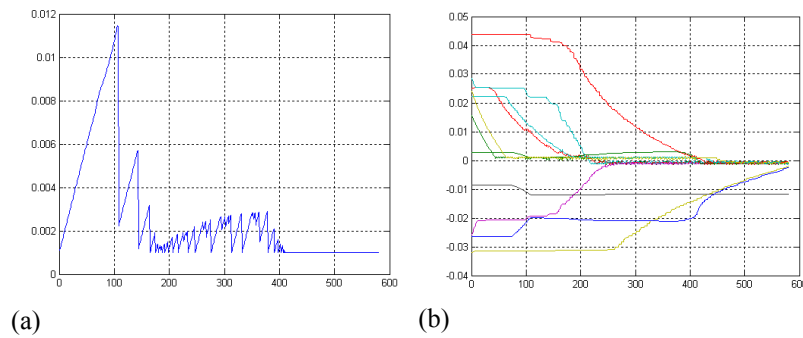


figure 12: The evolution of curvatures and  $\kappa_M$  when  $\Theta\{\kappa_M\}$  and  $\Theta\{B_\kappa\}$  are both active.